Cerebral Cortex August 2013;23:1923–1932
doi:10.1093/cercor/bhs178
Advance Access publication June 26, 2012

Modification of Visual Cortical Receptive Field Induced by Natural Stimuli

Yingjie Zhu[1,2] and Haishan Yao[1]

[1]Institute of Neuroscience, State Key Laboratory of Neuroscience, Shanghai Institutes for Biological Sciences, Chinese Academy of Sciences, Shanghai 200031, China and [2]Graduate School of Chinese Academy of Sciences, Shanghai 200031, China

Address correspondence to Haishan Yao. Email: haishanyao@ion.ac.cn

Visual experience can cause functional modification in the adult visual cortex; however, how cortical receptive fields (RFs) are dynamically modified by natural scene stimulation remains unclear. Here, using in vivo patch-clamp recordings from neurons in the rat primary visual cortex (V1), we showed that minutes of conditioning with natural movies could increase the similarity between cortical RF structure and the subset of movie images that depolarized the cell. This effect lasted for a few minutes in the absence of further movie stimulation. Manipulating the statistics of the movies by temporal shuffling or spatial whitening showed that the spatiotemporal correlation of the movie was important in inducing the RF modification. Furthermore, the movie-induced RF modification required the activation of *N*-methyl-D-aspartate receptors. Such rapid RF modification may play an important role in the dynamic coding of natural scenes.

Keywords: natural scenes, NMDA receptors, plasticity, primary visual cortex, spatiotemporal correlation

Introduction

Sensory experience plays an important role in shaping mammalian cortical circuits during both development and adulthood (Buonomano and Merzenich 1998; Gilbert 1998; Karmarkar and Dan 2006; Feldman 2009). For example, during the critical period, monocular deprivation causes a shift in ocular dominance in V1 (Wiesel and Hubel 1963) and a restructuring of geniculocortical arbors (Antonini and Stryker 1993), and early experience with moving visual stimuli has a significant impact on the development of cortical direction selectivity in visually naive animals (Li et al. 2008). During adulthood, the visual circuits can be modified by various manipulations, including perceptual learning (Schoups et al. 2001; Frenkel et al. 2006) and visual deprivation by retinal lesion (Kaas et al. 1990; Gilbert and Wiesel 1992). Adult cortical receptive field (RF) can also be modified at a time scale on the order of minutes by repetitive visual stimulation (Dragoi et al. 2000; Yao and Dan 2001; Fu et al. 2002) or by changing the statistics of visual stimuli (David et al. 2004; Sharpee et al. 2006).

Many forms of activity-dependent RF plasticity are likely mediated by synaptic modifications. For example, synchronous visual stimulation and iontophoretic cortical activation can change the orientation tuning and ocular dominance of V1 neurons (Frégnac et al. 1992; Shulz and Frégnac 1992). Synchronous stimulation of the RF and a region outside the RF can induce RF expansion toward the co-stimulated surround (Eysel et al. 1998). These effects are consistent with a Hebbian synaptic learning rule (Hebb 1949), according to which synaptic connection is strengthened when pre- and postsynaptic neurons are active simultaneously. Previous studies also revealed stimulus-timing-dependent changes in the cortical RF position and orientation tuning (Schuett et al. 2001; Yao and Dan 2001; Fu et al. 2002), which may be mediated by spike timing-dependent plasticity of synaptic connections (Bi and Poo 1998; Caporale and Dan 2008).

Although the aforementioned studies using artificial stimuli provided insight into the synaptic mechanism of experience-dependent RF modification, the effect of more natural sensory stimulation on adult cortical response remains poorly understood. A recent study in cat V1 showed that repeated stimulation with movies of natural scenes induced rapid improvement in response reliability and caused reverberation of the movie-evoked responses in spontaneous activity (Yao et al. 2007), but it remains unclear how RF is dynamically modified after movie stimulation and whether *N*-methyl-D-aspartate (NMDA) receptor-dependent synaptic plasticity is involved. Furthermore, it is not clear whether the movie-induced response modification (Yao et al. 2007) is due to the spatial or temporal correlations present in the movie. On the other hand, previous studies have shown that RFs measured with natural stimuli differed from those measured with artificial stimuli (David et al. 2004; Felsen et al. 2005; Sharpee et al. 2006), yet it is unclear whether natural stimuli cause RF changes that can be observed after the termination of natural stimulation or the RF difference is due to different mapping stimuli.

Using in vivo patch-clamp recordings from neurons in the rat primary visual cortex, we measured synaptic RFs before and after repetitive conditioning with movies of natural scenes. By changing the statistical properties of the conditioning stimuli, we were able to address whether RF modification depends on the spatiotemporal correlation of the stimulus. We showed that repetitive stimulation with natural movies caused enhancement and reduction in the amplitudes of visually evoked responses at different RF locations. After movie stimulation, the spatial structure of RF became more similar to the subset of movie images that depolarized the cell. This effect depended on the spatiotemporal correlation of the movie and required the activation of NMDA receptors. Furthermore, during movie conditioning, the spike rate to the preferred images of neurons selectively increased. Our results demonstrate that movie stimulation can cause rapid RF modification, which may enhance the stimulus selectivity of the neuron.

Materials and Methods

Surgery and Preparation

The use and care of animals complied with the guidelines of the Animal Advisory Committee at the Shanghai Institutes for Biological Sciences, and all the experiments were approved by the Animal Care and Use Committee at the Institute of Neuroscience, Chinese

Academy of Sciences (Shanghai, China). Adult Long-Evans rats (200–350 g) were anesthetized with an intraperitoneal injection of urethane (1.3 g/kg) or a mixture of fentanyl (0.3 mg/kg) and medetomidine (0.3 mg/kg). Additional doses were administered when needed. The animal was head fixed into a stereotaxic apparatus, with a stream of O_2 passing over the nose. Body temperature was maintained at 38° C with a heating blanket (FHC Inc.). A craniotomy (diameter 0.5 mm) was made above the right V1 (6.5–7.0 mm posterior to the bregma and 3.0–4.0 mm lateral to the midline), and the dura was removed. The left eye was fixed with a metal ring to prevent eye movement and occasionally irrigated with a sterile saline solution.

Recordings

Patch recordings were made with a MultiClamp 700B amplifier (Molecular Devices). Electrodes were pulled with a micropipette puller P-97 (Sutter Instrument) from unfilamented borosilicate glass (outer diameter: 1.5 mm; inner diameter: 0.8 mm, Sutter Instrument) to tips of 2 µm. The pipettes (4–7 MΩ) were filled with internal solution containing (in mM) K-gluconate 136.5, KCl 17.5, NaCl 9, $MgCl_2$ 1, 4-(2-hydroxyethyl)-1-iperazineethanesulfonic acid 10, and ethylene glycol tetraacetic acid 0.2 (pH 7.3 and mOsm 290). Amphotericin B (0.375 mg/mL, EMD Biosciences) was added before the experiment. The electrodes were inserted perpendicular to the cortical surface and advanced with a motorized micromanipulator (MX7600, Siskiyou). Visual responses were recorded in the current-clamp mode. The mean resting potential of the cells was −62.7 ± 8.0 mV (mean ± standard deviation [SD]).

For a subset of cells ($n = 24$ in Fig. 3*E*, $n = 15$ in Fig. 5*B–D*, $n = 48$ in Fig. 5*E*, $n = 26$ in Fig. 6*A*, $n = 48$ in Fig. 7*B*, and $n = 20$ in Fig. 7*C*), single-unit extracellular recordings were made with single tungsten microelectrodes (5 MΩ, A-M systems) or a 32-channel silicon probe (A4 × 8-5 mm-200-200-177, impedance 1.1–2.3 MΩ, NeuroNexus Technologies). The neural responses were amplified and filtered using an A-M systems Model 1800 amplifier or a Cerebus 128-channel system (Blackrock microsystems). Unit isolation was based on cluster analysis of waveforms. The data were sampled at 10 kHz by a Digidata 1440A digitizer (Molecular Devices) or at 30 kHz by the Cerebus 128-channel system. All the data were analyzed with the custom software in Matlab.

Visual Stimulation

Visual stimuli were presented with a 7″ LCD monitor (Xenarc Technologies Corp.; refresh rate 60 Hz; mean luminance 97.3 cd/m^2) placed 35 mm from the left (contralateral) eye. All the stimuli were updated every 2 frames, resulting in an effective frame rate of 30 Hz. The RF was mapped using sparse-noise stimuli, in which a white (or black) square (8.9°–11.2°) was flashed on a gray background at each of the 8 × 8 positions in a pseudorandom sequence. During movie conditioning, the RF was repetitively stimulated with a movie of time-varying natural scenes (van Hateren and Ruderman 1998). Each movie was 24.7 s long, containing 730 consecutive images (32 × 32 pixels, root mean square (RMS) contrast of 0.29) followed by 12 blank images. A total of 8 natural movies were used in this study. The mean luminance for each image in the conditioning stimuli was the same. Both the sparse-noise stimuli and the conditioning stimuli subtended 71.1° × 71.1°–90° × 90°.

To examine whether the spatiotemporal statistics of the conditioning stimuli influence RF modification, we also used 3 additional types of stimuli: Temporally shuffled movie, spatially whitened movie, and low-spatial-resolution white noise. To generate the shuffled movie, the images in the natural movie were temporally shuffled to remove temporal correlations. To generate the whitened movie, for each image in the natural movie, we randomized the spatial power spectrum by drawing the amplitude at each frequency randomly from a uniform distribution on [0 1]. In total, 6 shuffled movies and 6 whitened movies were used. For white noise conditioning, the movie images were replaced with 730 frames of spatiotemporal white noise (8 × 8 pixels, RMS contrast of 0.29). When we measured the responses of the same cell to the 4 types of conditioning stimuli (Fig. 5*A–D*), different stimuli were randomly interleaved and each stimulus was repeated 15 times.

RF Measurement, Conditioning, and Data Analysis

For each cell, we first mapped the RF using 50 or 75 repeats of sparse-noise stimuli. We then presented 5 blocks of conditioning and mapping stimuli. In each block, 5 repeats of movie stimuli (or other types of conditioning stimuli) were followed by 10 or 15 repeats of RF mapping stimuli. After each block of conditioning, 2 s of blank frames were presented to measure the spontaneous activity. The responses to the mapping stimuli in all the 5 blocks were averaged to obtain the RF after conditioning. The subthreshold (or spike) responses to sparse-noise stimuli were binned at 33.3 ms, and the spatiotemporal RFs (STRF) were computed using reverse correlation (Jones and Palmer 1987). To determine whether the response at a stimulus position was significant, we computed a baseline activity using the mean response within 0.5–1.5 s after stimulus onset at each position, and defined a threshold as 5 times SD above the baseline. For each stimulus position, the subthreshold (or spike) response was considered to be significant if the peak amplitude was above the threshold. For those positions at which the visual responses were significant, we compared the amplitudes of peak responses before and after the conditioning by computing the percent change in amplitude. For each cell, we computed the variance of the RF at each time delay and defined a signal-to-noise ratio (SNR) as the ratio of the maximum variance to the mean variance for RFs at delays 0.5–1.5 s after stimulus onset (Malone et al. 2007). For most cells, the SNRs for the ON and OFF regions were imbalanced, and the ON and OFF regions of the RF were largely overlapped (see Supplementary Material and Supplementary Fig. S1). To analyze the effect of conditioning, we picked the dominant RF region for each cell (Supplementary Material). Among the cells for which we measured RFs and analyzed the RF spatial profiles, only those with SNR >1.5 were included (patch recordings, $n = 133$; extracellular recordings, $n = 48$). The STRF was normalized to have unit variance and the spatial RF map at the delay with peak variance was used for further analysis.

To examine the relationship between RF modification and movie responses, we grouped the movie images into 3 subsets, S_+, S_o, and S_- images, by the following method. For the responses averaged over the last 2 blocks of conditioning (binned at the stimulus frame rate, 33.3 ms), we computed the mean and SD for the time bins above the mean potential, and defined an upper threshold as 1 SD above the mean (Fig. 3*A*, red dashed line). A lower threshold for the time bins below the mean potential was defined in a similar manner (Fig. 3*A*, blue dashed line). We defined those images that caused responses higher than the upper threshold as S_+ images, and those that caused responses lower than the lower threshold as S_- images. In addition to using 1 SD to define the upper and lower threshold, we also tried 0.75 SD and 1.25 SD in the analysis of RF modification (Supplementary Fig. S4). The third group of images, S_o, was defined as those images corresponding to the time bins within 0.25 SD of the mean potential (Fig. 3*A*, black dashed lines). In choosing the images for each group, we assumed that the response latency was 100 ms (corresponds to 3 frames). For the spatial RF measured before and after (RF_{before} and RF_{after}) movie stimulation, we computed the correlation coefficient (CC) between the RF and each image in the 3 groups. For each cell, we further computed the difference between the mean CC measured using RF_{after} and RF_{before} (defined as ΔCC), for each group of images.

To estimate the persistence of movie-induced RF modification, we mapped RF by 50 repeats of sparse noise every 3 min after the last block of conditioning and mapping, and computed the CC between the RF and each of the S_+ images. Because stable patch recordings could be sustained only for a limited time and the spike RF also showed similar modification as the synaptic RF (Fig. 3*D*), for this experiment we performed extracellular recordings ($n = 24$, 22, and 20 for the 3 time points in Fig. 3*E*, respectively) as well as patch recordings ($n = 43$, 16, and 13 for the 3 time points in Fig. 3*E*, respectively). For extracellular recordings, we included only those cells in which

both the SNR of RF >1.5 and the movie-evoked firing rate >1.5 spikes/s.

To define S_+ images for extracellular responses, we binned the movie-evoked peristimulus time histogram (PSTH) at the stimulus frame rate and set a threshold of 0.25 of the highest amplitude of the PSTH. Those images that caused extracellular responses higher than the threshold were defined as S_+ images. The reason to choose 0.25 for the threshold was that, for the subset of cells recorded intracellularly in which the movie-evoked firing rate >1.5 spikes/s ($n = 15$), the median firing rate for those bins corresponding to S_+ images was 0.25 of the maximum rate.

To analyze the spiking responses during the 5 blocks of movie conditioning, we set a threshold of 0.25 of the highest amplitude of the movie-evoked PSTH, and defined event (non-event) as those time bins that were above (below) the threshold.

To compare extracellular responses of the same cell to the 4 types of conditioning stimuli (Fig. 5*A–D*), the spike trains were binned at the stimulus frame rate (33.3 ms). To quantify the reliability of responses to repetitive conditioning, we computed the average between-trial CC for responses to the same stimulus. To quantify the degree of neural selectivity for the responses to each type of visual stimulus (Fig. 5*D*), we computed lifetime response sparseness *S*: $S = 1 - a$, where a denotes the activity fraction.

$$a = \frac{\left(\sum_i^n r_i/n\right)^2}{\sum_i^n r_i^2/n},$$

where n is the total number of time bins of the PSTH, and r_i is the firing rate at the i-th bin (Haider et al. 2010). As a nonparametric measure of neuronal selectivity, sparseness makes no assumption about the form of firing rate distribution, the tuning properties of the neuron, and the number of stimuli in the set (Rolls and Tovee 1995). For highly selective neurons (e.g., those respond to a single frame in the movie), *S* will approach 1. For nonselective neurons (e.g., those respond to all movie frames), *S* will approach 0.

Cortical Application of APV

To block the NMDA receptors, a standing pool of 1 mM D-2-amino-5-phosphonovaleric acid (APV) (Tocris Bioscience) was applied to the surface of primary visual cortex. We performed extracellular recordings to estimate the effect of APV application on spontaneous firing ($n = 26$, Fig. 6*A*) and movie-evoked responses ($n = 20$, Fig. 7*C*), and patch recordings ($n = 13$, Fig. 6*E*) to measure RF before and after movie conditioning in the presence of APV. For patch recordings, the spontaneous membrane potential responses of most cells showed visible hyperpolarization within 1 min of APV application. RF mappings and movie conditioning were performed after 5 min of APV application. To compensate for the hyperpolarization effect, a small amount of positive current (0–50 pA, depending on the degree of hyperpolarization and the input resistance of the cell) was injected to depolarize the cell to the potential before APV application. Only those cells whose membrane potential showed >2 mV hyperpolarization after APV application were included in the analysis.

Results

Movie-Stimulation-Induced Synaptic Modification in Receptive Field

RFs of V1 neurons were measured under current clamp with sparse noise (Fig. 1*A*,*B*) before and after repetitive visual stimulation with a movie of natural scene (see Materials and Methods). In many neurons, the movie-evoked responses showed sparse episodes of depolarization, which were reliable over trials (Fig. 1*B*). When the RF was measured again after the movie conditioning, we found that the peak response amplitudes were enhanced in some positions but reduced in other positions ($P < 0.01$, Wilcoxon rank-sum test, for all 4 positions marked with * in Fig. 1*B*). Over the population, movie stimulation induced significant changes ($P < 0.05$, Wilcoxon rank-sum test) in response amplitude for 1.5 ± 0.2 positions (or $26\% \pm 4\%$ positions; mean ± standard error of the mean [SEM]) in the RF (Fig. 2*A*,*B*). Among all the positions at which the responses were significant (see Materials and Methods), both reduction and enhancement in response amplitude were observed (Fig. 2*C*), indicating that movie stimulation caused disparate circuit modifications. To analyze the movie-induced RF change, we extracted the spatial profile of the RF at the time delay of maximum response (see Materials and Methods), and computed the CC between the spatial RF measured before and after movie stimulation (Fig. 2*D*). As a control, we also estimated the degree of spontaneous RF change after blank screen stimulation (same duration as the movie). The CC measured with movie conditioning was significantly smaller than that measured with blank control ($P < 0.0002$, Wilcoxon rank-sum test, Fig. 2*D*), indicating that the movie-induced RF change cannot be accounted for by the spontaneous fluctuations in the responses or the eye movements of the animal.

Increased Similarity Between Receptive Field and Movie Images

Previous studies showed that experience-dependent plasticity depends on the pattern of sensory inputs and the corresponding neural activity (Karmarkar and Dan 2006). Since the RF measured by sparse-noise stimuli could account for a small fraction of the movie-evoked responses (see Supplementary Material and Supplementary Fig. S2), we examined the relationship between RF modification and the movie responses. As seen from Figure 1*B*, the neuron was markedly depolarized in response to some images of the conditioning movie. According to the Hebb's rule, we reasoned that the synaptic inputs associated with depolarization may be strengthened, and RF measured after the conditioning may be more similar to those images that caused depolarization. To test this conjecture, we identified 3 groups of movie images, S_+, S_o, and S_- images, based on the movie-evoked membrane potential response (see Materials and Methods, Fig. 3*A*). Over the population, the responses evoked by S_+ and S_o images were 8.6 ± 0.5 and 2.3 ± 0.3 mV (mean ± SEM) above the mean spontaneous response, respectively, whereas the response evoked by S_- images was 2.3 ± 0.3 mV (mean ± SEM) below the spontaneous level (Supplementary Fig. S3). For each group of movie images, we measured the similarity of the image to RF_{before} (or RF_{after}) by CC. Figure 3*B*,*C* shows the probability distribution of CCs for 2 example cells, computed between RF (upper, RF_{before}; lower, RF_{after}) and each image in the 3 groups (red, S_+ images; black, S_o images; blue, S_- images). For both cells, the mean CC for S_+ images was higher for RF_{after} (Fig. 3*B*, CC = 0.1; Fig. 3*C*, CC = 0.38) than for RF_{before} (Fig. 3*B*, CC = 0.05; Fig. 3*C*, CC = 0.34), indicating an increase in similarity between S_+ images and RF structure after the movie conditioning. For each cell, we further computed a ΔCC, the difference between the mean CC measured using RF_{after} and RF_{before}, for each group of images. Over the population ($n = 43$), we found that ΔCC was significantly larger than zero for S_+ images ($P < 0.0005$, Wilcoxon signed-rank test) and S_o images ($P < 0.02$, Wilcoxon signed-rank

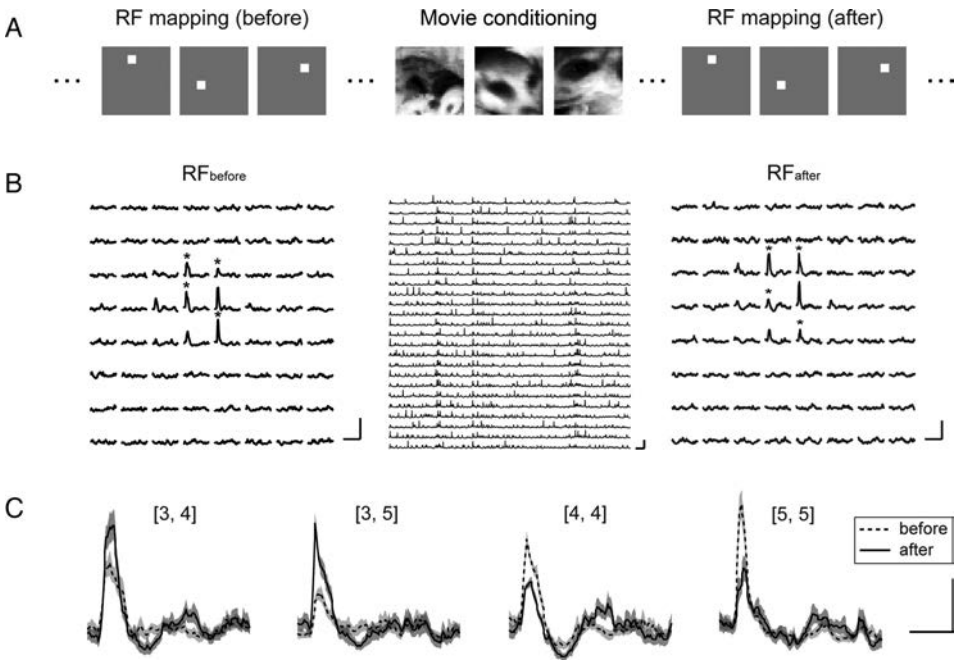

Figure 1. Movie-stimulation-induced modification in the amplitude of visual responses. (*A*) Left and right panel, sparse-noise stimuli used to map the RF before and after the movie conditioning. Middle panel, example movie images in the conditioning stimuli. (*B*) Left panel, synaptic RF of an example cell before movie conditioning. Scale bar: 15 mV, 500 ms. Middle panel, responses of the cell to repeated movie stimulation. Scale bar: 50 mV, 1 s. Right panel, the synaptic RF of the cell after movie conditioning. Scale bar: 15 mV, 500 ms. (*C*) Membrane potential responses (mean ± SEM) evoked by stimuli flashed at 4 different positions ([3, 4], [3, 5], [4, 4], [5, 5]) for the cell shown in (*B*), in which an asterisk is used to label each trace. Dashed curve, before movie stimulation. Solid curve, after movie stimulation. Shaded region: SEM. Scale bar: 5 mV, 200 ms.

test), but not for S_- images ($P = 0.15$, Wilcoxon signed-rank test, Fig. 3*D* left panel). This indicates that the spatial profile of synaptic RF became more similar to S_+ and S_o images after movie stimulation. To reduce the arbitrariness in choosing the upper (lower) threshold used to define S_+ (S_-) images (see Materials and Methods), we repeated the analysis of Figure 3*D* using another 2 different thresholds and found that ΔCC remained significant for S_+, but not for S_- images (Supplementary Fig. S4). For cells in which both the synaptic RF and the spike RF were measured, when we performed the analysis using the spike RF, we found that ΔCC was significantly larger than zero only for the S_+ images ($P < 0.05$, Wilcoxon signed-rank test, $n = 29$, Fig. 3*D*, right panel). This result is consistent with the effect that spike threshold serves to enhance feature selectivity of cortical neurons (Priebe and Ferster 2008). To examine the persistence of RF modification, we continued to map RF in the absence of further movie conditioning (see Materials and Methods). We found that the effect of movie conditioning persisted for several minutes (Fig. 3*E*). The rapid decay of RF modification may be due to the spontaneous activity or spiking activity evoked by the mapping stimuli, which can reverse activity-induced synaptic modifications in vivo (Zhou et al. 2003).

Dependence of RF Modification on the Spatiotemporal Correlation of Conditioning Stimulus

Natural scenes exhibit significant correlations in space and time (Field 1987; Dong and Atick 1995). To examine whether the RF modification depends on the spatiotemporal characteristics of the conditioning stimuli, we also tested the effect using 3 additional types of stimuli: Temporally shuffled movie, in which the images in the natural movie were temporally shuffled; spatially whitened movie, in which the pixels in each image were spatially uncorrelated; and low-spatial-resolution white noise (see Materials and Methods). For white noise stimuli, we used a spatial resolution lower than that of natural movie so that the stimuli could effectively drive the neurons (Supplementary Fig. S5). When we measured the effect of the 3 types of conditioning stimuli on synaptic RF, we found that none of them induced significant change in CC (Fig. 4*A*–*C*), indicating that both the spatial and the temporal correlations of the conditioning stimulus are important in inducing the RF modification.

Why do natural movie conditionings induce RF modification more efficiently than the other types of visual stimuli? To address this question, we compared the response properties to natural movies with those to other stimuli. The mean membrane potential to natural movies was not significantly different from that to each of the 3 types of stimuli (Fig. 4*D*, $P > 0.4$ for all the 3 comparisons, Wilcoxon rank-sum test). The reliability of membrane potential response (see Materials and Methods) to whitened movies, however, was significantly lower than that to natural movies ($P < 0.01$, Wilcoxon rank-sum test), whereas the reliability to shuffled movies (or white noise) was not significantly different from that to natural movies (Fig. 4*E*, $P > 0.2$ for shuffled movies, $P > 0.3$ for white noise, Wilcoxon rank-sum test). To further examine the response difference, we made extracellular recordings to measure the responses of each cell to the 4 types of stimuli (see Materials and Methods). As shown in the example in Figure 5*A*, both the firing rate and the temporal structure of this neuron's responses appeared different to the 4 stimuli. Over the population ($n = 15$), we found that the mean firing

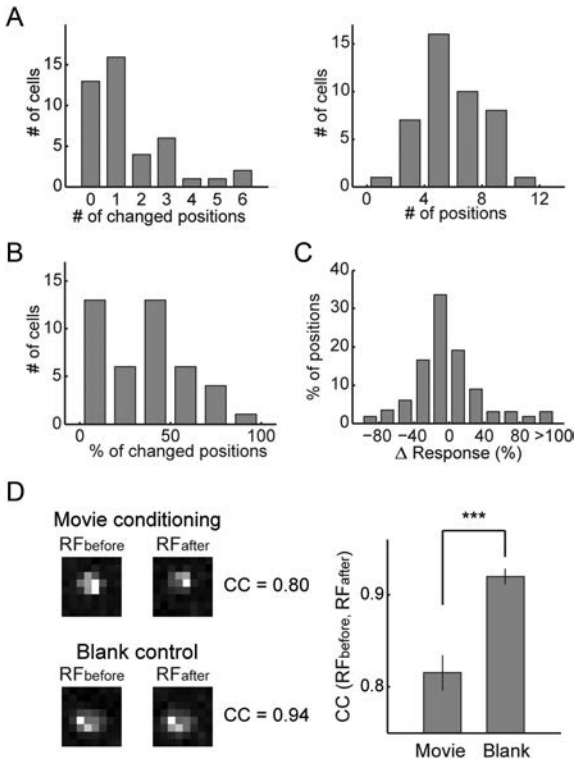

Figure 2. Movie-induced modification of synaptic RFs for a population of neurons. (*A*) Left, distribution of the number of stimulus positions that showed significant change in response amplitude after movie conditioning. Right, distribution of the number of positions that showed significant visual response ($n = 43$). (*B*) Distribution of the percent of stimulus positions that showed significant change in response amplitude after movie conditioning. (*C*) Distribution of the percent change in response amplitude for all cells, computed using those stimulus positions at which the responses were significant. (*D*) Left panel, the spatial RF measured before and after movie stimulation for an example cell (upper); spatial RF measured before and after blank stimulation for another example cell (lower). Right panel, mean CC (mean ± SEM) between RF measured before and after movie (or blank) stimulation. $***P < 0.001$, Wilcoxon rank-sum test (movie, $n = 43$; blank, $n = 19$).

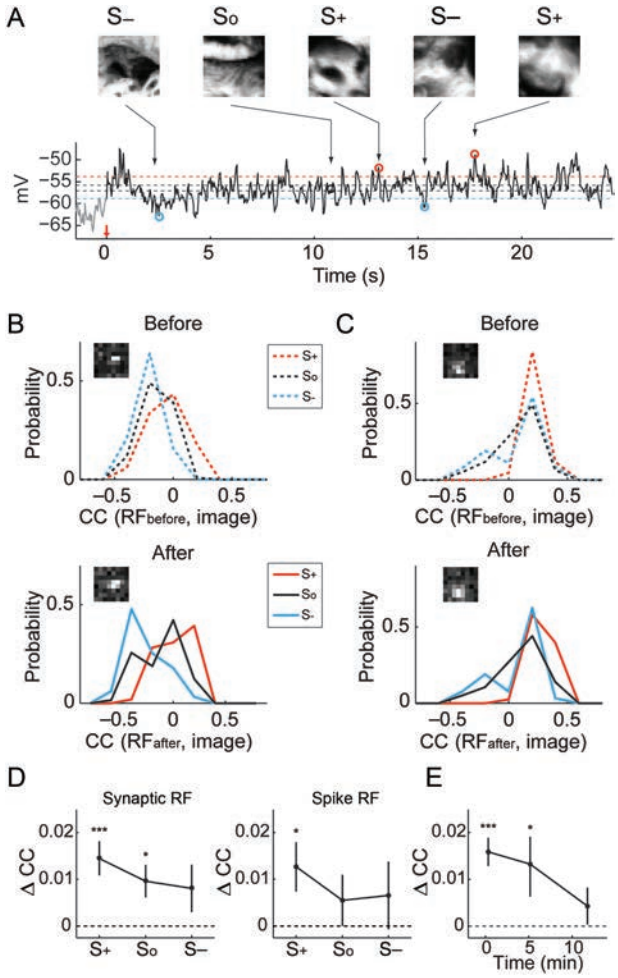

Figure 3. RF measured after movie conditioning was more similar to the subset of movie images that caused depolarization. (*A*) Bottom panel shows an example cell's membrane potential response averaged over the last 2 blocks of movie conditioning. The red arrow marks the onset of movie stimulation. The gray trace before time 0 was spontaneous membrane potential response. Three groups of movie images, S_+, S_o, and S_- (example images are illustrated in the top panel), can be identified based on the movie-evoked membrane potential response. Red dashed line, upper threshold. S_+ images were defined as those that caused responses above the upper threshold. Blue dashed line, lower threshold. S_- images were those that caused responses below the lower threshold. Images corresponding to the responses within the 2 black dashed lines were S_o images. (*B*) Distribution of CCs between RF (inset) and each group of the movie images for an example cell. Upper panel, CCs computed using RF_{before}. Lower panel, CCs computed using RF_{after}. Red, S_+ images; black, S_o images; blue, S_- images. (*C*) Distribution of CCs between RF (inset) and each group of the movie images for another example cell. Conventions as in (*B*). (*D*) ΔCC, the difference in mean CC computed using RF_{after} and RF_{before}, for each of the 3 groups of movie images. Left panel, RFs were measured with membrane potential response ($n = 43$). Right panel, RFs were measured with spiking response ($n = 29$, a subset of those cells in the left panel). $***P < 0.001$; $*P < 0.05$; Wilcoxon signed-rank test. (*E*) The increased in CC for S_+ images persisted for a few minutes in the absence of further movie conditioning ($n = 67$, 38, and 33 for each time point). $***P < 0.001$; $*P < 0.05$; Wilcoxon signed-rank test. Error bars are ±SEM.

rate to whitened movies was significantly lower than that to natural movies ($P < 0.00005$, Wilcoxon signed-rank test), whereas the mean rate to shuffled movies (white noise) was higher than (similar to) that to natural movies (Fig. 5*B*). The reliability of response to whitened movies was significantly lower than that to natural movies ($P < 0.0002$, Wilcoxon signed-rank test), whereas the reliability to shuffled movies (white noise) was similar to that to natural movies (Fig. 5*C*). This indicates that whitened movies did not drive the neurons as efficiently as natural movies. We next determined what other aspect of the responses may exhibit difference between natural movie and shuffled movie (or white noise) stimulation. Visual inspection of the example cell in Figure 5*A* shows that the spikes appeared in fewer frames under the stimulation of natural movie compared with shuffled movie or white noise, suggesting a difference in neuronal selectivity for different stimuli. To quantify the degree of selectivity, we used the measure of lifetime sparseness (see Materials and Methods). Sparseness approaches 1 for highly selective neurons and approaches 0 for nonselective neurons. Over the population, the response sparseness was significantly higher for natural movies than for shuffled movies ($P < 0.0002$, Wilcoxon signed-rank test) or white noise ($P < 0.0002$, Wilcoxon signed-rank test, Fig. 5*D*). Although the response sparseness for whitened movies was similar to that for natural movies ($P > 0.5$, Wilcoxon signed-rank test, Fig. 5*D*), this was likely due to the lower firing rate to whitened movies. When we further examined the relationship between the response sparseness and RF modification, we found that ΔCC for S_+ images was correlated with the sparseness of movie-evoked response ($r = 0.37$, $P < 0.01$, Fig. 5*E*). Thus, the effectiveness of natural

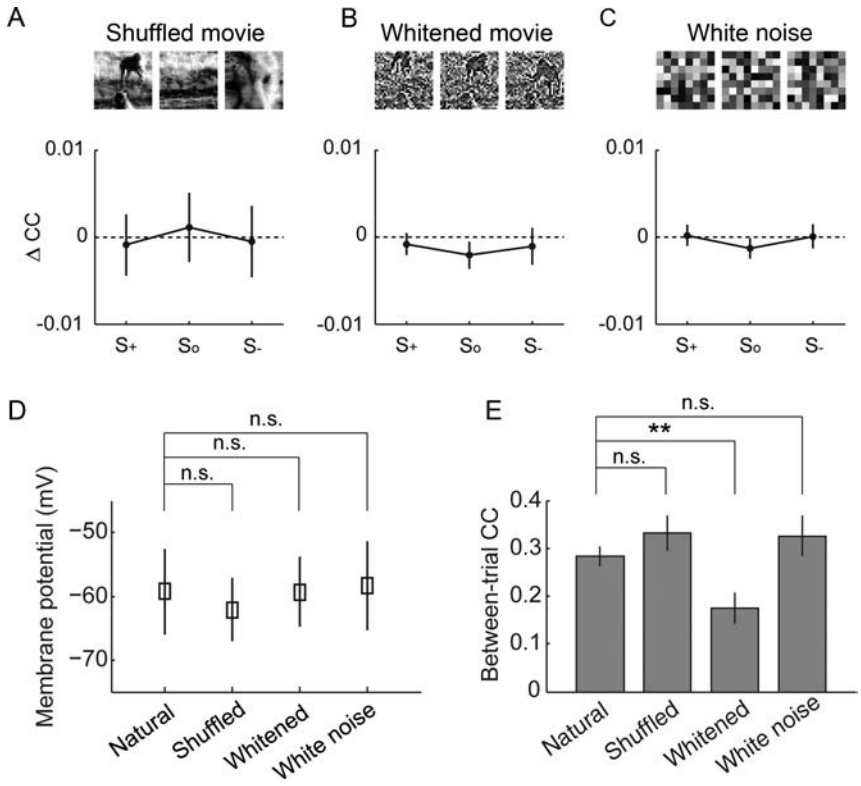

Figure 4. Effect of 3 other types of conditioning stimuli on RF change. (*A*) ΔCC induced by shuffled movie conditioning ($P > 0.4$ for any of the 3 groups of images, $n = 21$, Wilcoxon signed-rank test). Top panel, example images in the stimuli. (*B*) ΔCC induced by whitened movies ($P > 0.2$, $n = 14$). (*C*) ΔCC induced by white noise ($P > 0.1$, $n = 13$). (*D*) Comparison of membrane potential response to natural movies and that to each of the 3 types of conditioning stimuli. (*E*) Comparison of response reliability measured by the average between-trial CC (**$P < 0.01$, Wilcoxon rank-sum test). Error bars are ±SEM.

movies at inducing RF modification may be partially accounted for by the higher degree of response sparseness.

Dependence of RF Modification on NMDA Receptors

Many forms of activity-dependent synaptic modification require activation of NMDA receptors (Bear 1996; Malenka and Nicoll 1999; Dan and Poo 2004). To test whether the mechanism underlying movie-induced RF changes involves NMDA receptor-dependent synaptic plasticity in the cortex, we locally applied NMDA receptor antagonist APV to the visual cortex (see Materials and Methods). Previous in vivo studies showed that APV application could cause significant reduction in both the spontaneous and visually evoked activity (Fox et al. 1989; Miller et al. 1989). In our study, we found that the spontaneous firing rate decreased by ~50% a few minutes after APV (1 mM) application and the effect lasted at least 30 min (Fig. 6*A*). Patch recordings showed that the spontaneous membrane potential was hyperpolarized by -4.4 ± 2.2 mV (mean ± SD) after the application of APV (Fig. 6*B*). To compensate for the effect of hyperpolarization, we injected a small amount of depolarizing current during RF mappings and natural movie conditioning (see Materials and Methods), which ensured that the movie stimuli could evoke robust depolarization and spiking responses in the presence of APV (Fig. 6*C*). While the movie-evoked responses were reliable and sparse, the probability distributions of CCs were similar between RF_{before} and RF_{after} (Fig. 6*D*). Across the population, ΔCC was not significantly different from zero for any of the 3 groups of movie images ($P > 0.3$, Wilcoxon signed-rank test, $n = 13$, Fig. 6*E*). Thus, the movie-induced RF modifications depend on the activation of NMDA receptors.

Selective Increase in Spike Response to Movie Images

Since the RF became more similar to the S_+ images, we wondered whether repetitive stimulation with natural movies could enhance the image selectivity of the neuron. We thus examined the firing rate of the neurons over the 5 blocks of movie conditioning (see Materials and Methods). Because S_+ images that caused depolarization often evoked high firing rates, we divided the time bins of the movie-evoked PSTH into event bins (Fig. 7*A*, red) and non-event bins (Fig. 7*A*, blue) (see Materials and Methods). Presumably, the event spikes were evoked by the S_+ images that the neuron preferred and the non-event spikes by the non-S_+ images. Over the population ($n = 48$), we found a marked increase in the number of event spikes over the 5 blocks of movie stimulation, but no significant change in the spikes of non-events (Fig. 7*B*). Thus, consistent with the increased similarity between the spike RF and the S_+ images (Fig. 3*D*, right), repetitive movie stimulation induced a preferential increase in the responses to the preferred images, resulting in enhanced stimulus selectivity of the neurons. When we applied APV to the visual cortex, neither event spikes nor non-event spikes showed significant change over time ($n = 20$, Fig. 7*C*), further suggesting that the movie-induced modifications require the action of NMDA receptors.

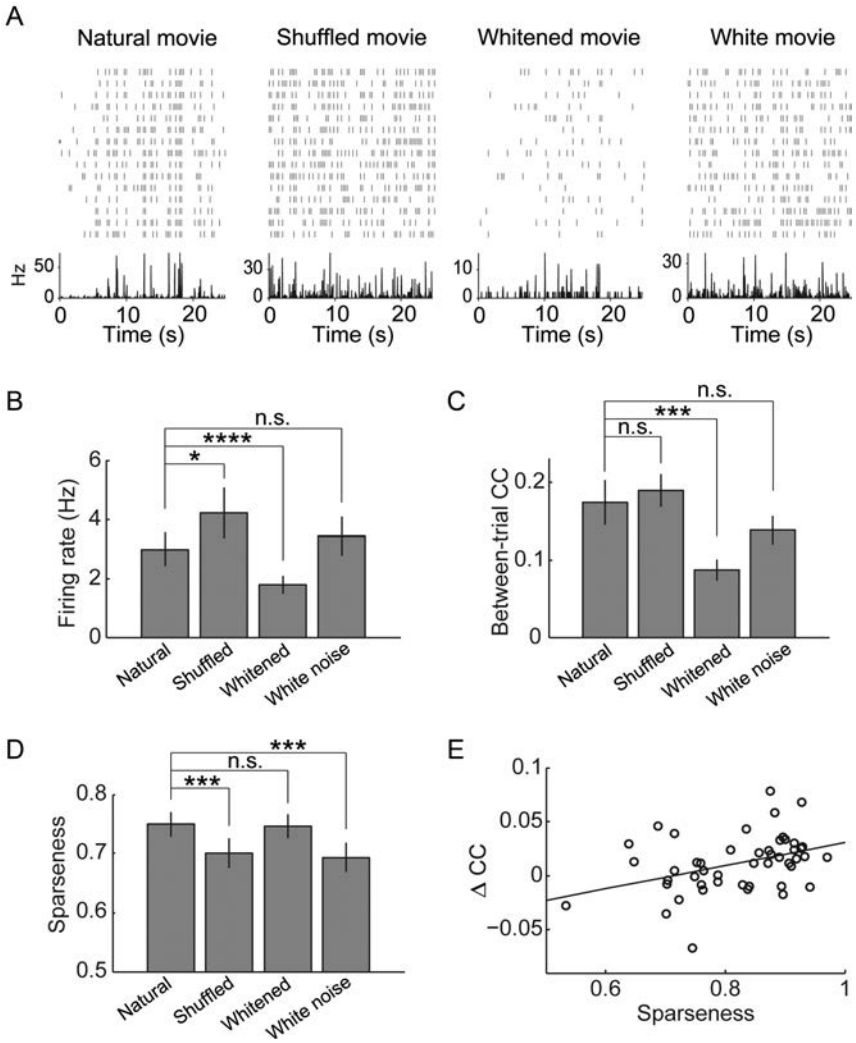

Figure 5. Comparison of response properties to different visual stimuli. (*A*) Spiking responses of an example cell to repetitive stimulation of natural movie, shuffled movie, whitened movie, and white noise. Lower panel shows the PSTH to each type of stimuli. (*B*) Comparison of mean firing rate to natural movies and that to each of the 3 types of visual stimuli (****$P < 0.0001$; *$P < 0.05$, $n = 15$, Wilcoxon signed-rank test). (*C*) Comparison of response reliability measured by the average between-trial CC (***$P < 0.001$, Wilcoxon signed-rank test). (*D*) Comparison of response sparseness (***$P < 0.001$, Wilcoxon signed-rank test). (*E*) The sparseness of movie-evoked response versus change in CC for S_+ images ($r = 0.37$, $P < 0.01$, $n = 48$). Solid line is the linear fit of the data. Error bars are ±SEM.

Discussion

We have shown that repetitive movie stimulation caused an increase in similarity between the RF structure and the subset of movie images that depolarized the cell. This RF change is consistent with the Hebbian synaptic learning rule (Hebb 1949), which can account for several forms of cortical RF modification induced by visual stimulation (Eysel et al. 1998; Eyding et al. 2002; Fu et al. 2002). Whereas several previous studies of RF plasticity have controlled the precise timing of spikes or manipulated the postsynaptic activity in response to sensory stimulation (Frégnac et al. 1992; Shulz and Frégnac 1992; Cruikshank and Weinberger 1996; Yao and Dan 2001; Fu et al. 2002; Yao et al. 2004; Meliza and Dan 2006; Dahmen et al. 2008), the RF modification in the current study was induced under a more natural stimulation condition. The movie-induced RF modification may contribute to the experience-dependent enhancement in stimulus selectivity of cortical neurons.

To examine whether the Hebb's rule can account for the RF modification, we constructed a Hebbian neural network model to perform further analysis (Supplementary Material). The model consisted of a single postsynaptic neuron driven by 32 × 32 presynaptic neurons (Supplementary Fig. S6*A*), and synaptic modifications were implemented on the basis of the correlation between pre- and post-synaptic spiking activity (Dayan and Abbott 2001). We simulated a total of 43 postsynaptic neurons, and set each RF_{before} to be those measured from the cells in Figure 3*D*. We found that the model could predict the RF changes observed in the experiment (Supplementary Fig. S6*C–E*), supporting the notion that RF modification is mediated by Hebbian synaptic plasticity.

We found that RF modification depended on the activation of NMDA receptors, further suggesting activity-dependent synaptic modification as the underlying synaptic mechanism. Because the APV was locally applied to the cortical surface, the synapses modified by movie stimulation were likely to be the intracortical connections. Intracortical connections have been shown to contribute significantly to shaping cortical RFs (Gilbert 1998; Fu et al. 2002), and various forms of plasticity have been demonstrated at synapses of intracortical

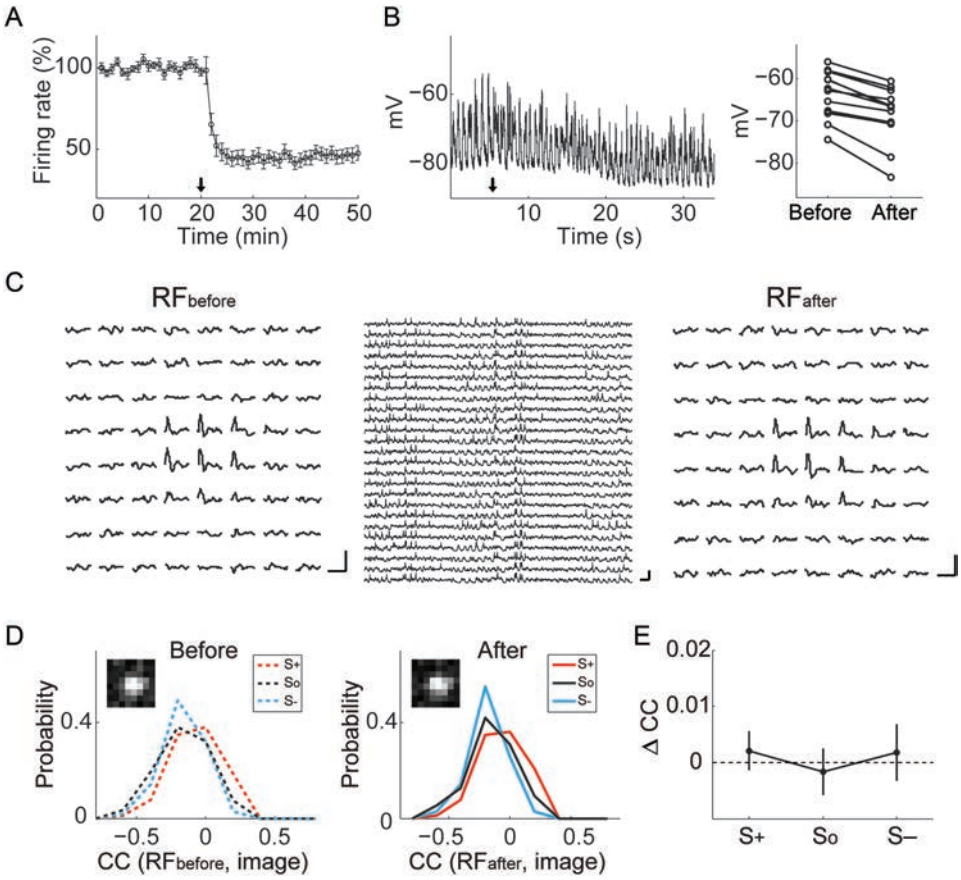

Figure 6. RF modification depended on the activation of NMDA receptors. (*A*) Spontaneous firing rate of 26 cells before and after application of 1 mM APV in the visual cortex. Arrow indicates the time of APV application. (*B*) Left, spontaneous membrane potential response of an example cell before and after application of 1 mM APV in the visual cortex. Arrow indicates the time of APV application. Right, mean membrane potential before and 2 min after APV application ($n = 13$). (*C*) Left, RF of an example cell measured before movie conditioning. Scale bar: 10 mV, 500 ms. Middle, responses of this neuron to repetitive conditioning of a natural movie. Scale bar: 50 mV, 1 s. Right, RF of this neuron measured after movie conditioning. Scale bar: 10 mV, 500 ms. All measurements were done in the presence of APV. (*D*) Left, distribution of CCs between RF_{before} (inset) and movie images for the example cell in (*C*). Right, distribution of CCs between RF_{after} (inset) and movie images. Red, S_+ images; black, S_o images; blue, S_- images. (*E*) ΔCC induced by movie conditioning in the presence of APV ($P > 0.3$ for each group of the movie images, Wilcoxon signed-rank test, $n = 13$). Error bars are ±SEM.

connections in visual cortical slices (Hirsch and Gilbert 1993; Sjostrom et al. 2001; Froemke and Dan 2002). Previous studies showed that stimulus-timing-dependent orientation plasticity can be transferred interocularly (Schuett et al. 2001; Yao et al. 2004), suggesting that these effects are mainly mediated by intracortical connections. It is of interest for future study to further investigate whether the sites of movie-induced synaptic modifications occur mainly at intracortical connections or at the feedforward thalamic connections.

The movie-induced change in RF spatial profile resulted from a combination of enhancement and reduction in the amplitudes of local synaptic responses at different RF locations. A similar effect has been reported in previous studies of RF plasticity in the rat visual cortex (Meliza and Dan 2006) and tadpole tectum (Vislay-Meltzer et al. 2006), cortical frequency tuning in the auditory system (Dahmen et al. 2008), and the whisker-evoked responses in the barrel cortex (Jacob et al. 2007). The effects observed in these studies may reflect the spread of long-term potentiation or long-term depression to neighboring synapses (Engert and Bonhoeffer 1997; Fitzsimonds et al. 1997; Tao et al. 2001) as well as the overlapping populations of presynaptic neurons activated by the sensory stimulus. In our study, the heterogeneous changes in the amplitude of local synaptic responses may be due to the complex spatiotemporal pattern of movie images. Assuming that these images activated converging synaptic inputs to the postsynaptic neuron, the excitatory inputs that were associated with the depolarization and spiking of the postsynaptic neuron may be potentiated, and those that were not correlated with the postsynaptic depolarization may be depressed.

We showed that manipulating the statistics of natural scenes movies by temporal shuffling (spatial whitening) or using white noise as conditioning stimuli could diminish the RF modification. Responses to whitened movies showed lower firing rates and lower reliability compared with those to natural movie stimulation. Thus, the failure of whitened movies to induce RF changes may simply be due to its low efficacy in driving the cortical neurons. While the analysis of firing rate and response reliability demonstrated that shuffled movies (or white noise) could drive the cells as well as natural movies, the sparseness of spiking response to natural movies was significantly higher than that to shuffled movies (or white noise). Furthermore, the sparseness of movie-evoked response was significantly correlated with the degree of RF modification, suggesting that response

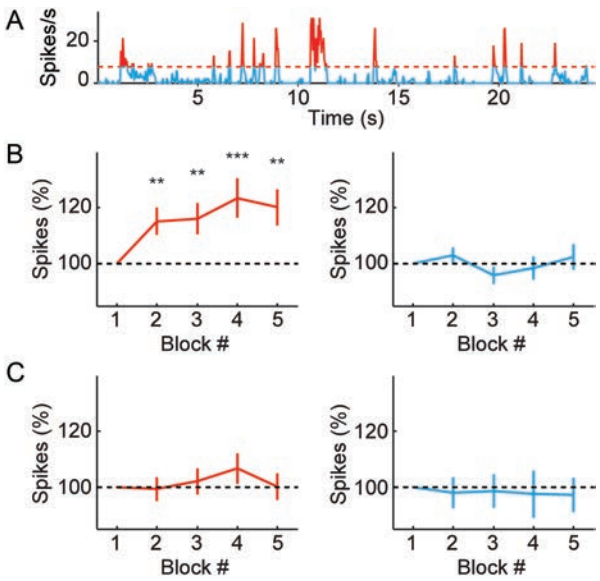

Figure 7. Selective increase in spike response to natural movie images. (*A*) PSTH of an example cell in response to natural movie conditioning. Red dashed line indicates the threshold used to define the event bins. Red and blue, event and non-event bins, respectively. (*B*) Number of spikes normalized by that in the first block of movie conditioning for event bins (left) and non-event bins (right), averaged from 48 cells (**$P < 0.01$, ***$P < 0.001$, Wilcoxon signed-rank test). (*C*) Number of event spikes (left) and non-event spikes (right) for cells measured in the presence of APV ($n = 20$). Error bars are ±SEM.

sparseness may play an important role in inducing RF modification. Our result also suggests that the sparse cortical response evoked by natural stimulation (Vinje and Gallant 2000; Haider et al. 2010) may contribute to the mechanism underlying the adaptation of the visual system to efficient coding of natural scenes (Attneave 1954; Barlow 1961; Simoncelli and Olshausen 2001).

Supplementary Material

Supplementary material can be found at: http://www.cercor.oxfordjournals.org/.

Funding

This work was supported by 973 program (2011CBA00405) and the Hundred Talents Program of the Chinese Academy of Sciences.

Notes

We thank Y. Dan for discussions and critical comments on the manuscript. We also thank H. Zhong and W. Xu for their technical assistance. *Conflict of Interest*: None declared.

References

Antonini A, Stryker MP. 1993. Rapid remodeling of axonal arbors in the visual cortex. Science. 260:1819–1821.
Attneave F. 1954. Some informational aspects of visual perception. Psychol Rev. 61:183–193.
Barlow HB. 1961. Possible principles underlying the transformation of sensory messages. In: Rosenblith WA, editors. Sensory communication. Cambridge (MA): MIT Press. p. 217–234.
Bear MF. 1996. A synaptic basis for memory storage in the cerebral cortex. Proc Natl Acad Sci USA. 93:13453–13459.
Bi GQ, Poo MM. 1998. Synaptic modifications in cultured hippocampal neurons: dependence on spike timing, synaptic strength, and postsynaptic cell type. J Neurosci. 18:10464–10472.
Buonomano DV, Merzenich MM. 1998. Cortical plasticity: from synapses to maps. Annu Rev Neurosci. 21:149–186.
Caporale N, Dan Y. 2008. Spike timing-dependent plasticity: a Hebbian learning rule. Annu Rev Neurosci. 31:25–46.
Cruikshank SJ, Weinberger NM. 1996. Receptive-field plasticity in the adult auditory cortex induced by Hebbian covariance. J Neurosci. 16:861–875.
Dahmen JC, Hartley DE, King AJ. 2008. Stimulus-timing-dependent plasticity of cortical frequency representation. J Neurosci. 28:13629–13639.
Dan Y, Poo MM. 2004. Spike timing-dependent plasticity of neural circuits. Neuron. 44:23–30.
David SV, Vinje WE, Gallant JL. 2004. Natural stimulus statistics alter the receptive field structure of v1 neurons. J Neurosci. 24:6991–7006.
Dayan P, Abbott LF. 2001. Theoretical neuroscience. Cambridge (MA): The MIT Press.
Dong DW, Atick JJ. 1995. Statistics of natural time-varying images. Network. 6:345–358.
Dragoi V, Sharma J, Sur M. 2000. Adaptation-induced plasticity of orientation tuning in adult visual cortex. Neuron. 28:287–298.
Engert F, Bonhoeffer T. 1997. Synapse specificity of long-term potentiation breaks down at short distances. Nature. 388:279–284.
Eyding D, Schweigart G, Eysel UT. 2002. Spatio-temporal plasticity of cortical receptive fields in response to repetitive visual stimulation in the adult cat. Neuroscience. 112:195–215.
Eysel UT, Eyding D, Schweigart G. 1998. Repetitive optical stimulation elicits fast receptive field changes in mature visual cortex. Neuroreport. 9:949–954.
Feldman DE. 2009. Synaptic mechanisms for plasticity in neocortex. Annu Rev Neurosci. 32:33–55.
Felsen G, Touryan J, Han F, Dan Y. 2005. Cortical sensitivity to visual features in natural scenes. PLoS Biol. 3:e342.
Field DJ. 1987. Relations between the statistics of natural images and the response properties of cortical cells. J Opt Soc Am A. 4:2379–2394.
Fitzsimonds RM, Song HJ, Poo MM. 1997. Propagation of activity-dependent synaptic depression in simple neural networks. Nature. 388:439–448.
Fox K, Sato H, Daw N. 1989. The location and function of NMDA receptors in cat and kitten visual cortex. J Neurosci. 9:2443–2454.
Frégnac Y, Shulz D, Thorpe S, Bienenstock E. 1992. Cellular analogs of visual cortical epigenesis. I. Plasticity of orientation selectivity. J Neurosci. 12:1280–1300.
Frenkel MY, Sawtell NB, Diogo AC, Yoon B, Neve RL, Bear MF. 2006. Instructive effect of visual experience in mouse visual cortex. Neuron. 51:339–349.
Froemke RC, Dan Y. 2002. Spike-timing-dependent synaptic modification induced by natural spike trains. Nature. 416:433–438.
Fu YX, Djupsund K, Gao H, Hayden B, Shen K, Dan Y. 2002. Temporal specificity in the cortical plasticity of visual space representation. Science. 296:1999–2003.
Gilbert CD. 1998. Adult cortical dynamics. Physiol Rev. 78:467–485.
Gilbert CD, Wiesel TN. 1992. Receptive field dynamics in adult primary visual cortex. Nature. 356:150–152.
Haider B, Krause MR, Duque A, Yu Y, Touryan J, Mazer JA, McCormick DA. 2010. Synaptic and network mechanisms of sparse and reliable visual cortical activity during nonclassical receptive field stimulation. Neuron. 65:107–121.
Hebb DO. 1949. The organization of behavior: a neuropsychological theory. New York: John Wiley.
Hirsch JA, Gilbert CD. 1993. Long-term changes in synaptic strength along specific intrinsic pathways in the cat visual cortex. J Physiol. 461:247–262.
Jacob V, Brasier DJ, Erchova I, Feldman D, Shulz DE. 2007. Spike timing-dependent synaptic depression in the in vivo barrel cortex of the rat. J Neurosci. 27:1271–1284.

Jones JP, Palmer LA. 1987. The two-dimensional spatial structure of simple receptive fields in cat striate cortex. J Neurophysiol. 58:1187–1211.
Kaas JH, Krubitzer LA, Chino YM, Langston AL, Polley EH, Blair N. 1990. Reorganization of retinotopic cortical maps in adult mammals after lesions of the retina. Science. 248:229–231.
Karmarkar UR, Dan Y. 2006. Experience-dependent plasticity in adult visual cortex. Neuron. 52:577–585.
Li Y, Van Hooser SD, Mazurek M, White LE, Fitzpatrick D. 2008. Experience with moving visual stimuli drives the early development of cortical direction selectivity. Nature. 456:952–956.
Malenka RC, Nicoll RA. 1999. Long-term potentiation—a decade of progress? Science. 285:1870–1874.
Malone BJ, Kumar VR, Ringach DL. 2007. Dynamics of receptive field size in primary visual cortex. J Neurophysiol. 97:407–414.
Meliza CD, Dan Y. 2006. Receptive-field modification in rat visual cortex induced by paired visual stimulation and single-cell spiking. Neuron. 49:183–189.
Miller KD, Chapman B, Stryker MP. 1989. Visual responses in adult cat visual cortex depend on N-methyl-D-aspartate receptors. Proc Natl Acad Sci USA. 86:5183–5187.
Priebe NJ, Ferster D. 2008. Inhibition, spike threshold, and stimulus selectivity in primary visual cortex. Neuron. 57:482–497.
Rolls ET, Tovee MJ. 1995. Sparseness of the neuronal representation of stimuli in the primate temporal visual cortex. J Neurophysiol. 73:713–726.
Schoups A, Vogels R, Qian N, Orban G. 2001. Practising orientation identification improves orientation coding in V1 neurons. Nature. 412:549–553.
Schuett S, Bonhoeffer T, Hubener M. 2001. Pairing-induced changes of orientation maps in cat visual cortex. Neuron. 32:325–337.
Sharpee TO, Sugihara H, Kurgansky AV, Rebrik SP, Stryker MP, Miller KD. 2006. Adaptive filtering enhances information transmission in visual cortex. Nature. 439:936–942.
Shulz D, Frégnac Y. 1992. Cellular analogs of visual cortical epigenesis. II. Plasticity of binocular integration. J Neurosci. 12:1301–1318.
Simoncelli EP, Olshausen BA. 2001. Natural image statistics and neural representation. Annu Rev Neurosci. 24:1193–1216.
Sjostrom PJ, Turrigiano GG, Nelson SB. 2001. Rate, timing, and cooperativity jointly determine cortical synaptic plasticity. Neuron. 32:1149–1164.
Tao HW, Zhang LI, Engert F, Poo M. 2001. Emergence of input specificity of ltp during development of retinotectal connections in vivo. Neuron. 31:569–580.
van Hateren JH, Ruderman DL. 1998. Independent component analysis of natural image sequences yields spatio-temporal filters similar to simple cells in primary visual cortex. Proc Biol Sci. 265:2315–2320.
Vinje WE, Gallant JL. 2000. Sparse coding and decorrelation in primary visual cortex during natural vision. Science. 287: 1273–1276.
Vislay-Meltzer RL, Kampff AR, Engert F. 2006. Spatiotemporal specificity of neuronal activity directs the modification of receptive fields in the developing retinotectal system. Neuron. 50:101–114.
Wiesel TN, Hubel DH. 1963. Single-cell responses in striate cortex of kittens deprived of vision in one eye. J Neurophysiol. 26: 1003–1017.
Yao H, Dan Y. 2001. Stimulus timing-dependent plasticity in cortical processing of orientation. Neuron. 32:315–323.
Yao H, Shen Y, Dan Y. 2004. Intracortical mechanism of stimulus-timing-dependent plasticity in visual cortical orientation tuning. Proc Natl Acad Sci USA. 101:5081–5086.
Yao H, Shi L, Han F, Gao H, Dan Y. 2007. Rapid learning in cortical coding of visual scenes. Nat Neurosci. 10:772–778.
Zhou Q, Tao HW, Poo MM. 2003. Reversal and stabilization of synaptic modifications in a developing visual system. Science. 300: 1953–1957.